

ORIGINAL ARTICLE

Cholestane isolated from green seaweeds inhibits biofilm formation in *A. baumannii*: A Molecular Modeling Study

Babini CK,^{1,2} Reena A,^{1*} Malathi Kullappan,³ and Krishna Mohan Surapaneni⁴

¹PG and Research Department of Microbiology, Mohamed Sathak College of Arts and Science, Sholinganallur, Chennai.

²Kumararani Meena Muthiah College of Arts and Science, Adyar, Chennai.

³Department of Research, Panimalar Medical College Hospital & Research Institute, Chennai.

⁴Departments of Biochemistry, Medical Education, Clinical Skills & Simulation, Research, Panimalar Medical College Hospital & Research Institute, Chennai.

*Corresponding Author- reena.denzil@yahoo.com

ABSTRACT

Acinetobacter baumannii (*A. baumannii*), a Gram-negative, non-fermentative, and non-motile coccobacillus, belongs to the Moraxellaceae family. The organism forms biofilms on both biotic and abiotic surfaces and causes nosocomial infections, including urinary tract infections (UTIs). It is one of the ESKAPE pathogens associated with multidrug-resistant hospital-acquired infections. *Acinetobacter baumannii* is one of the Priority pathogens listed among the Bacterial Priority Pathogen List (BPPL) by WHO. Recent studies emphasize that resistance to carbapenem and colistin is emerging in *A. baumannii*. Biofilm formation is a vital virulent factor of AMR. The matrix surrounding the bacteria in biofilm becomes tolerant to harsh conditions, leading to unsuccessful antibiotic treatments. Therefore, there is an urgent need for alternative therapies to control biofilm development and inhibit *A. baumannii* adherence on biotic and abiotic surfaces. Marine seaweeds have been explored for their potential bioactivity. Among the three types of seaweeds, edible green seaweeds were minimally studied. In the current study, a molecular docking analysis was conducted to identify potential inhibitors targeting *A. baumannii* protein *CsuE* and DNA gyrase, among 14 compounds predicted from the methanolic extract of edible green seaweeds, *Codium tomentosum* and *Ulva lactuca* via GC/MS. Results showed that cholestane exhibited greater binding energies of -10.25 kcal/mol and -9.55 kcal/mol, respectively. Consequently, cholestane may serve as a promising inhibitor against biofilm-forming *A. baumannii*.

Keywords: *A. baumannii*, cholestane, Biofilm, *Codium*, *Ulva* and Docking

Received 13.02.2026

Revised 24.02.2026

Accepted 26.03.2026

How to cite this article:

Babini CK, Reena A, Malathi K, and Krishna Mohan S Cholestane isolated from green seaweeds inhibits biofilm formation in *A. baumannii*: A Molecular Modeling Study. Adv. Biores., Vol 17 (3) March 2026: 50-59.

INTRODUCTION

Antimicrobial resistance is one of the major global concerns in disease management, and complicates treatment. AMR has increased the incidence of common diseases like community-acquired UTIs, Nosocomial Urinary infections, respiratory illness, and septicemia. *Acinetobacter baumannii*, an opportunistic, aerobic, non-motile, nonspore-forming gram-negative coccobacillus responsible for hospital-acquired and community-acquired infections [1-2]. *Acinetobacter baumannii* is one of the top three Priority pathogens listed in the Bacterial Priority Pathogen List (BPPL) by WHO [3]. Microorganisms adopt various strategies to develop antimicrobial resistance. The Biofilm-forming ability of an organism increases the persistence of microorganisms on biotic or abiotic surfaces for a prolonged period. The architecture of biofilm facilitates a conducive environment for bacteria to survive in adverse conditions like exposure to antimicrobial substances and development of resistance [4]. *A. baumannii* employs various strategies to combat the effect of antibiotics, including β -lactamase production, modification of the target site, efflux pumps, and permeability defects. Ayobami *et al*, reported that 20.9% and 13.6% of nosocomial infections are caused by *A. baumannii* and carbapenem-resistant *A. baumannii*, respectively [5]. According to the National Institutes of Health (NIH) and the Center for

Disease and Prevention (CDP), about 80% of bacterial infections in humans are associated with biofilm [6].

The formation of biofilm was influenced by various physical and environmental factors. The major factors that mediate irreversible attachment are CsuE, ompA, and FimH. Chen *et al* exposed that CSU pilus contributes to the adhesion of bacteria to respiratory epithelial cells. In order to develop novel compounds from natural sources for therapy, Csu pili can be utilized as a target protein [7].

Several natural resources are explored for the development of new antimicrobial agents. Plants and marine flora are employed in drug discovery. Seaweeds are a vast resource explored by many researchers to find new antimicrobial substances. Among the seaweeds (red, brown, and green), green edible seaweeds *Codium tomentosum* and *Ulva lactuca* were employed for the current study. The metabolites of both the seaweeds were analyzed by GC/MS and metabolomics. Further, the lead components were applied to identify their antibiofilm activity *In-Silico* molecular docking method.

MATERIAL AND METHODS

Sample Collection and Preparation.

Two different live edible green seaweeds were collected from the coastal region of Mandapam, (Latitude 9.283945°, Longitude 79.178559°) Ramanathapuram, Tamilnadu, India. The Seaweeds were thoroughly washed, shade-dried, and ground to a fine powder for further processing. The live samples were verified and identified as *Codium tomentosum* Stackhouse and *Ulva lactuca* by the authenticated Botanist, Central National Herbarium, Botanical Survey of India, Howrah, India.

Extraction Preparation

The Soxhlet extraction of powdered *Codium tomentosum* and *Ulva lactuca* was carried out using Methanol, a polar solvent. The extracts were concentrated by a rotary evaporator and stored for analysis.

GC/MS Analysis and Metabolomic Study.

The Samples (methanol extract) in the triplet CMB 1, CMB2, CMB3 (*C. tomentosum*) and UMB 1, UMB2, UMB3 (*Ulva lactuca*) were evaluated for the untargeted metabolites by GC-MS QP2010 Plus Model Shimadzu (Toshvin Analytical). The mass spectrum of the unknown component was compared with the spectrum of the known components stored in the NIST 14s.lib (National Institute of Standards and Technology) library.

The GC-MS data of metabolites of CMB (1-3) and UMB (1-3) samples were analyzed by Metabo Analyst 5.0. The data were statistically scrutinized with fold change analysis and T-test to identify the lead metabolites from CMB and UMB.

Molecular Modeling

Among the 50 top lead components identified in fold-change and T-test analysis, fourteen common components (Table. 1) were selected for the current molecular docking against two vital proteins associated with biofilm formation in *Acinetobacter baumannii*.

Preparation of Protein

The three-dimensional (3D) crystal structures of CsuE (PDB: 6FJY) and DNA gyrase subunit B (PDB: 7PQM) of *A. baumannii* [8, 9] were retrieved from the protein data bank (PDB)¹⁰ maintained by the research laboratory for structural bioinformatics (RCSB). Both structures were crystallized through the X-ray diffraction method with the resolution of 2.31 Å and 1.55 Å, respectively. The co-crystallized non-residue atoms, ions, and metals were detached from the protein structures.

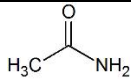
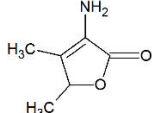
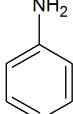
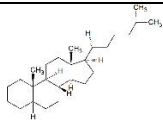

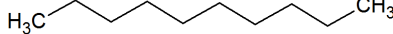
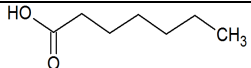
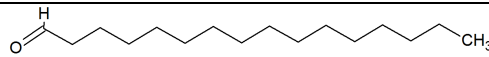
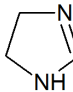

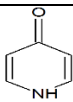
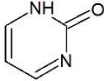
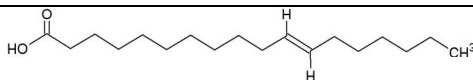
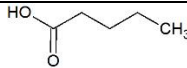
Active Site Prediction

The active site amino acids of CsuE and DNA gyrase subunit B of *A. baumannii* were retrieved from the literature [8-10].

Ligands

The 3D structures of phytoconstituents isolated from the methanolic extracts of green seaweeds were obtained from the PubChem chemical database of the National Center for Biotechnology Information (NCBI) [11] (Table 1).

Table 1- GC/MS spectrum predicted compounds isolated from the methanolic extract of green seaweed

S. No.	PubChem ID	Predicted compounds	Structure
1	178	Acetamide	
2	6421106	3-Amino-4,5-dimethyl-2(5H)-furanone	
3	6115	Aniline	
4	6857534	Cholestane	
5	6351	Cyclopropane	
6	15600	Decane	
7	8094	Heptanoic Acid	
8	984	Hexadecanal	
9	68156	Imidazoline	
10	8141	Nonane	
11	3111	Pyridone	
12	386209230	Pyrimidinone	
13	5281127	Vaccenic Acid	
14	7991	Valeric Acid	

Molecular Docking Studies

The AutoDock 4.2.6 version was utilized to find the binding orientation of protein and ligand. Here, phytochemicals isolated from the green seaweed were docked with the target proteins, CsuE and DNA

gyrase subunit B of *A. baumannii*. The structures of proteins and compounds were processed through AutoDock Tools and used in PDBQT format. For CsuE and DNA gyrase, the grid box points were fixed as 100 x 100 x 100 for x, y, and z directions with 0.375 Å grid spacing to cover the active sites. Along with all the required parameters, the AutoGrid run was executed to produce the grid map and desolvation map. Finally, the AutoDock run was carried out, and the protein-ligand complex was saved in PDB format. The empirical scoring function was expressed in kcal/mol.

RESULTS AND DISCUSSION

GC/MS Analysis and Metabolomic Study.

GC/MS analysis revealed 1368 components in CMB and UMB samples. These data were analysed for the identification of lead components common to both samples. Fold change and T-test analysis identified the Top 50 components present in the CMB and UMB samples. Furthermore, fourteen common components were selected, and their binding efficacy was examined using by Docking (Table. 2)

Active sites:

The active sites of CsuE (Glu24, Thr307, Gln309, Asp187, Tyr302, Asn267, Tyr217 & Phe312) and DNA gyrase subunit B (Asp87, Arg90, Thr179, Ile92, Arg150, Ile108 & Ala104) of *A. baumannii* was obtained through literature review [8, 9] (Figure 1 and Figure 2).

Molecular docking studies

The analysis of the binding mode of compounds isolated from the green seaweed with csuE of *A. baumannii* reveals that csuE-cholestane has the best binding affinity complex, selected based on the binding energy. The csuE-cholestane interaction energy was found to be -10.25 kcal/mol (Table 2). Here, cholestane does not form any hydrogen bonds with csuE (Figure 3 (a)), whereas it has formed hydrophobic interaction with sixteen polar and non-polar amino acids namely, Ala185, Val306, Met206, Phe285, Thr305, Gln186, Ser205, Ile247, Tyr245, Val188, Asp304, Asn189, Met234, Asp187, Gln303 and Tyr302 (Figure 3 (b)). At this point, non-polar amino acids buried inside the protein stabilize the protein structure by restricting water interaction.

From the literature study, it was evident that cholestane, as a derivative, possesses anti-microbial activity. A group of 3 α -amino-5 α -cholestane and 3 α ,7 α -diamino-5 α -cholestane derivatives with imidazole and pyridine rings showed antibacterial activity against Methicillin-resistant *Staphylococcus aureus* (MRSA) pathogens. In particular, 3 α ,7 α -Di-(pyridylmethyl) amino-5 α -cholestane derivative inhibits *Staphylococcus epidermidis* with the MIC value of 1 μ g/ml [11]. In another study, 2'-amino-5 α -cholest-6-eno [6,5-d] oxazole derivatives exhibited good inhibitory activity against Gram-positive (*Bacillus subtilis*, *Streptococcus pyogenes* & *Staphylococcus aureus*), Gram-negative (*Pseudomonas aeruginosa*, *Escherichia coli* & *Salmonella typhimurium*) and five different fungal strains (*Candida albicans*, *Candida glabrata*, *Penicillium spp.*, *Fusarium oxysporium* and *Aspergillus niger*) [12].

Cholestane derivatives also act as an anti-cancer agent; an oxysterol called cholestane-3 β , 5 α , 6 β -triol exhibits anti-cancer activity against human prostate cancer cells. It dose-dependently suppressed the proliferation in DU-145, PC-3 and LNCaP CDXR-3 cell lines [13].

Subsequent, the csuE-pyridone complex was found to have -6.91kcal/mol binding energy and formed five hydrogen bonds with Ser258, Gly257, Arg255, Arg262 & Lys249, where the bond distances fall within 1.7 Å to 2.3 Å respectively (Figure 4) (Table 2). Synthesis of benzimidazole bearing 2-pyridone derivatives possesses both anti-bacterial and anti-fungal activity [14].

In the third position, the csuE-nonane complex was selected with a binding energy of -5.27 kcal/mol and thirteen hydrophobic interactions (Met234, Thr192, Thr301, Phe190, Gly191, Tyr302, Leu243, Gly300, Leu199, Ile297, Phe195, Ala299 & Pro298). The H-bond formation was not observed between csuE and nonane (Figure 5).

Synthesized *N*-acyl-2,4,6,8-tetraphenyl-3,7-diazabicyclo [3.3.1] nonanes possess anti-bacterial activity against Gram-positive bacteria (*Staphylococcus aureus*) and Gram-negative bacteria (*Salmonella paratyphi*, *Escherichia coli*, *Proteus vulgaris* and *Serratia marcescens*) [15]. Anti-biofilm compound isolated from *Nocardiosis sp.* strain DMS 2 (MH900226), 1, 4-diaza-2, 5-dioxo-3-isobutyl bicycle [4.3.0] nonane, shown inhibitory activity against biofilm-forming *Klebsiella pneumoniae* [16].

The docking of csuE with other compounds like vaccenic acid, hexadecanal, heptanoic acid, amino-4,5-dimethylfuranone, valeric acid and decane results in the binding energy falling within the range of -5.26 to -4.18 kcal/mol. A few other compounds, namely, aniline, pyrimidinone, acetamide, imidazoline and cyclopropane show their interaction energies within the range of -3.99 to -2.13 kcal/mol.

Similarly, the molecular docking of DNA gyrase subunit B with green seaweed extract phytoconstituents predicts DNA gyrase-cholestane as the best complex with the binding energy of -9.55 kcal/mol. The hydrogen bond interaction was not observed and fourteen hydrophobic interactions with the amino acids

Ala61, Arg90, Asn60, Asp87, Gly89, Gly91, Glu64, Ile92, Ile108, His113, Thr179, Val85, Val57 and Val181 (Figure 6) (Table 3). The second position was occupied by vaccenic acid with the binding affinity of -5.23 kcal/mol. The DNA gyrase-vaccenic acid complex was found with one hydrogen bond (Arg150 (2.1 Å)) and twelve hydrophobic contacts (Arg90, Pro93, Glu64, Gly91, Ile92, Asn60, Asp87, Val181, Val57, Thr179, Ala61 & Val85) (Figure 7). The *cis* and *trans* vaccenic acid express anti-bacterial and anti-biofilm activity against *Pseudomonas aeruginosa* with MIC of 128-256 µg/mL and MBIC of 8-512 µg/mL [17]. Also, vaccenic acid inhibits quorum sensing in *Chromobacterium violaceum* and MRSA [18].

The *in silico* study conducted by El-Zairy et al in 2024 [19] reveals that molecular docking of vaccenic acid against thymidylate kinase of *Staphylococcus aureus* subsp. *aureus* MRSA252 and DNA gyrase of *E.coli* using Molsoft software yielded -91.76 kcal/mol & -96.27 kcal/mol of binding energies, respectively.

The DNA gyrase-hexadecanal complex was in the third place with -4.78 kcal/mol binding energy, two hydrogen bond interactions (Gly91 (3.1 Å) & Arg150 (2.3 Å)) and twelve hydrophobic interactions (Val134, Ile108, Ala61, Ile92, Thr179, Glu64, Gly91, Pro93, Arg90, Asn60, Val57 & Asp87) (Figure 8). Previous study on *Dorema ammoniacum* roots exposes that hydrodistillation of the plant root yielded pale yellow oil with β-bisabolene (15.1%), hexadecanal (13.2%) and (E)-nerolidol (11.3%) as the leading contents and the oil was found to exhibit antibacterial activity against *Shigella dysenteriae*. Similarly, the chloroform and ethyl acetate extract of the root inhibits *Bacillus subtilis*, *Pseudomonas aeruginosa* and *Staphylococcus aureus* [20].

Table 2- Molecular docking results for Csue of *A. baumannii* and compounds isolated from the methanolic extract of *C.tomentosum* and *U.lactuca*

S.No.	Compounds	Binding energy (kcal/mol)	Amino acids involved in hydrogen bond interaction and distance (Å)	Hydrophobic interaction
1.	Cholestane	-10.25	-	Ala185, Val306, Met206, Phe285, Thr305, Gln186, Ser205, Ile247, Tyr245, Val188, Asp304, Asn189, Met234, Asp187, Gln303 and Tyr302
2.	Pyridone	-6.91	Ser258 (1.9), Gly257 (2.1), Arg255 (1.7), Arg262 (2.1) and Lys249 (2.3)	Asn222, Arg262, Asn230 and Trp256
3.	Nonane	-5.27	-	Met234, Thr192, Thr301, Phe190, Gly191, Tyr302, Leu243, Gly300, Leu199, Ile297, Phe195, Ala299, Pro298
4.	Vaccenic Acid	-5.26	Asp304 (1.7 & 2.1)	Met234, Val188, Gln303, Gly191, Phe190, Tyr302, Ala193, Ala196, Leu199, Gly300, Pro298, Ile297
5.	Hexadecanal	-4.63	ASP304 (1.8 & 3.0)	Met206, Phe285, Val308, Leu220, Ile247, Gln186, Tyr245, Val188, Val306 and Gln303
6.	Heptanoic Acid	-4.44	Lys249 (1.7), Ser264 (2.0), Asn267 (1.9) and Arg262 (1.8)	Trp263, Ser252, Asn250 and Asp254
7.	Amino-4,5-Dimethylfuranone	-4.32	Lys249 (2.0), Arg262 (2.2), Ser264 (1.9), Asn267 (2.2)	Trp263, Tyr217, Arg262
8.	Valeric Acid	-4.36	Lys249 (1.7), Arg262 (1.9), Ser264 (2.0) and Asn267 (1.8)	Trp263 and Asn250
9.	Decane	-4.18	-	Leu243, Ala299, Pro298, Tyr302, Thr192, Phe195, Leu199, Ala193, Gly300, Thr301, Phe190 and Met234
10.	Aniline	-3.99	Gly191 (2.0) and Thr192 (2.1)	Gly300, Phe190, Met234, Leu199, Thr301 and Tyr302
11.	Pyrimidinone	-3.57	Tyr302 (2.0)	Ala193, Gly300, Thr301, Gly191, Phe190, Leu199 and Thr192
12.	Acetamide	-3.21	Thr296 (1.8) and Ile297 (2.2)	Phe195, Asp291, Thr296 and Ile289
13.	Imidazoline	-2.75	Thr192 (2.1) and Tyr302 (2.1)	Leu199, Gly300, Ala193 and Thr301
14.	Cyclopropane	-2.13	-	Tyr302, Gly300, Phe195, Ala299, Leu199 and Pro298

There are many studies in line with our work, the bioactive components (2-pentadecanone, 6,10,14-trimethyl-, hexadecenoic acid, methyl ester, n-hexadecanoic acid, 1,2-benzenedicarboxylic acid, and mono(2-ethylhexyl) ester) isolated from *Sargassum sp.* (brown algae) possess anti-*Staphylococcus sp.* activity with MIC and MBC ranging from 6.25–12.5 mg/L to 50–>50 mg/mL, respectively. It also inhibits biofilm formation in *Staphylococcus spp.* [21]. Also, glycolipid biosurfactants isolated from *Shewanella algae B12* inhibit bacterial pathogens and preformed biofilms in *Bacillus cereus* (83%), *Streptococcus pneumoniae* (53%), *Pseudomonas aeruginosa* (92%), *Escherichia coli* (64%), *Klebsiella pneumoniae* (87%), and *Acinetobacter sp.* (72%) [22].

Table 3 - Molecular docking results for DNA gyrase and compounds isolated from the methanolic extract of *C. tomentosum* and *U.lactuca*

S.No.	Compounds	Binding energy (kcal/mol)	Amino acids involved in hydrogen bond interaction and distance (Å)	Hydrophobic interaction
1.	Cholestane	-9.55	-	Gly89, Val85, Arg90, Thr179, Glu64, Ala61, Asp87, Val57, Val181, Ile92, Gly91, Asn60, His113 and Ile108
2.	Vaccenic Acid	-5.23	Arg150 (2.1)	Arg90, Pro93, Glu64, Gly91, Ile92, Asn60, Asp87, Val181, Val57, Thr179, Ala61 and Val85
3.	Pyrimidinone	-4.78	Arg28 (2.2 & 2.9), Gly29 (2.7), Leu30 (2.0), Arg34 (1.9 & 2.0) and Asp163 (3.2)	Arg28, Pro164, Thr110, Gly162 and Asp163
4.	Hexadecanal	-4.76	Gly91 (3.1) and Arg150 (2.3)	Val134, Ile108, Ala61, Ile92, Thr179, Glu64, Gly91, Pro93, Arg90, Asn60, Val57 and Asp87
5.	Amino-4,5-Dimethylfuranone	-4.45	Asn60 (2.5), Ser135 (1.7), Ile108 (2.1) and Ile111 (2.3)	Asn60, Ile108, Gly133, His113, Val132
6.	Decane	-4.45	-	Gly91, Arg90, Glu64, Val57, Asp87, Val85, Ala61, Asn60, Thr179 and Ile92
7.	Nonane	-4.18	-	Arg90, Gly91, Asn60, Ile92, Val157, Val85, Ala61, Val181, Asp87 and Glu64
8.	Pyridone	-4.03	Ile111 (2.2), Asn60 (2.2 & 3.3) and Val134 (2.2)	Val132, Gly133, Ser135, His113, Ile108
9.	Aniline	-3.87	Ser103 (1.8) and Glu106 (1.8)	Pro167, Val102, Leu168 and Ile96
10.	Heptanoic Acid	-3.66	Gly29 (1.8) and Arg28 (1.9 & 1.9)	Gly29, Thr110, Val107, Ile111, Glu100, Glu106, Val102
11.	Acetamide	-3.53	Ile108 (2.2), Ile111 (1.9), Ser135 (2.4) and His113 (1.9)	Leu112, Val132, Gly133, Ser135 and Val134
12.	Valerate	-3.12	Arg28 (1.8 & 1.9) and Gly29 (2.0)	Gly29, Thr110, Pro164, Asp163, Gly162
13.	Imidazoline	-2.94	Ser103 (2.1) and Glu106 (1.9)	Ile96, Pro167, Val102 and Leu168
14.	Cyclopropane	-2.14	-	Val57, Thr179, Asp87, Val181, Ala61 and Val85

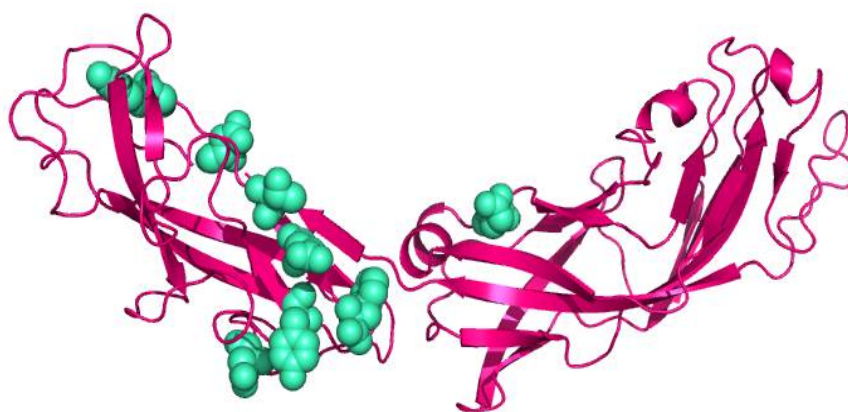


Figure 1. Active site region (spheres) of csuE (cartoon) of *A. baumannii*

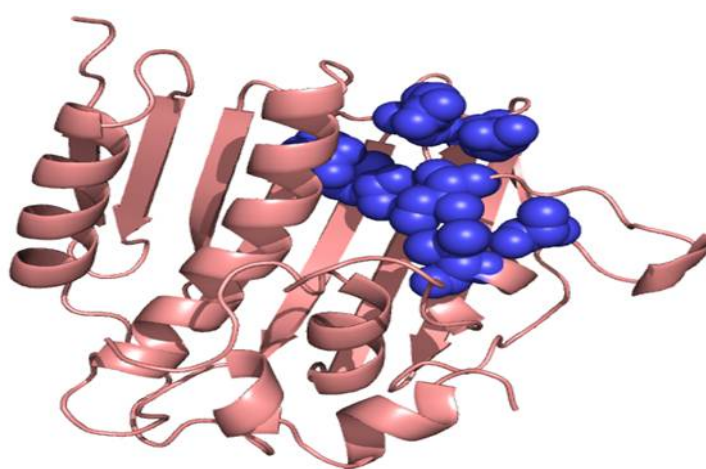


Figure 2. Active site region (spheres) of DNA gyrase (cartoon) of *A. baumannii*

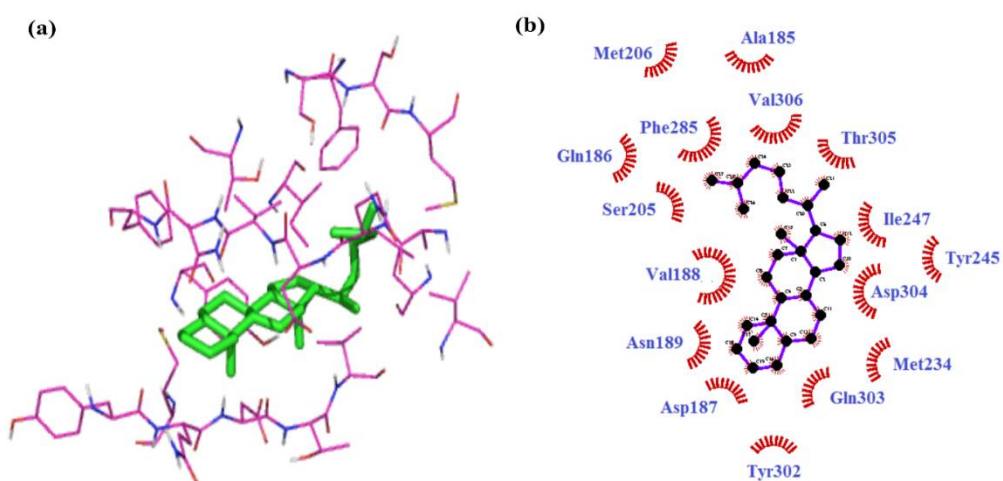


Figure 3. Docking results for csuE of *A. baumannii* and cholestane. (a) Binding mode of cholestane with the active site of csuE. Hydrogen bond interactions were not observed, and the residues around the compound were highlighted. (b) Hydrophobic interactions of cholestane with csuE

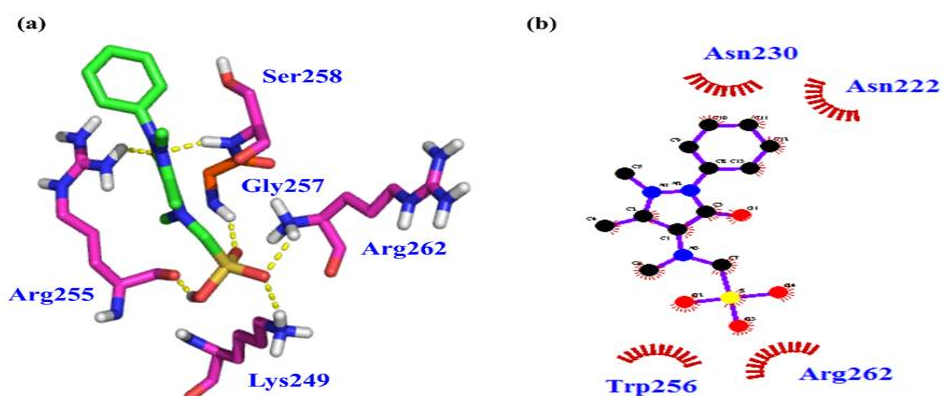


Figure 4. Docking results for csuE of *A. baumannii* and pyridone. (a) Binding mode of pyridone with the active site of csuE. (b) Hydrophobic interactions of pyridone with csuE

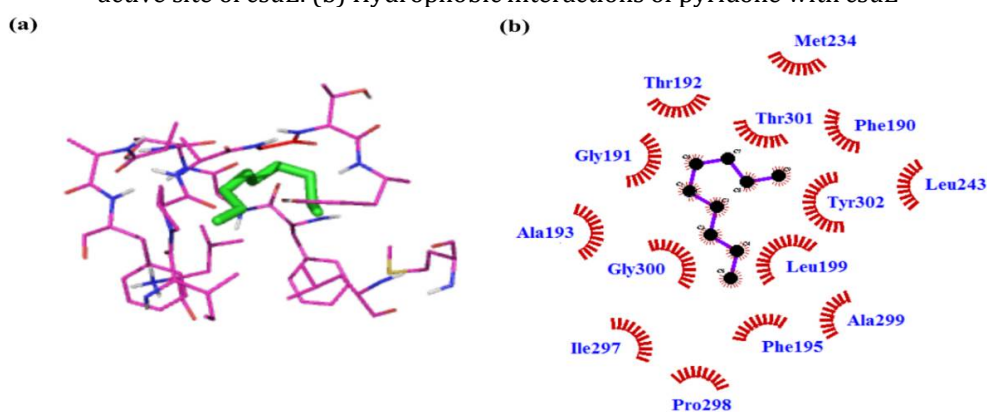


Figure 5. Docking results for csuE of *A. baumannii* and nonane. (a) Binding mode of nonane with the active site of csuE. Hydrogen bond interactions were not observed and the residues around the compound were highlighted. (b) Hydrophobic interactions of nonane with csuE

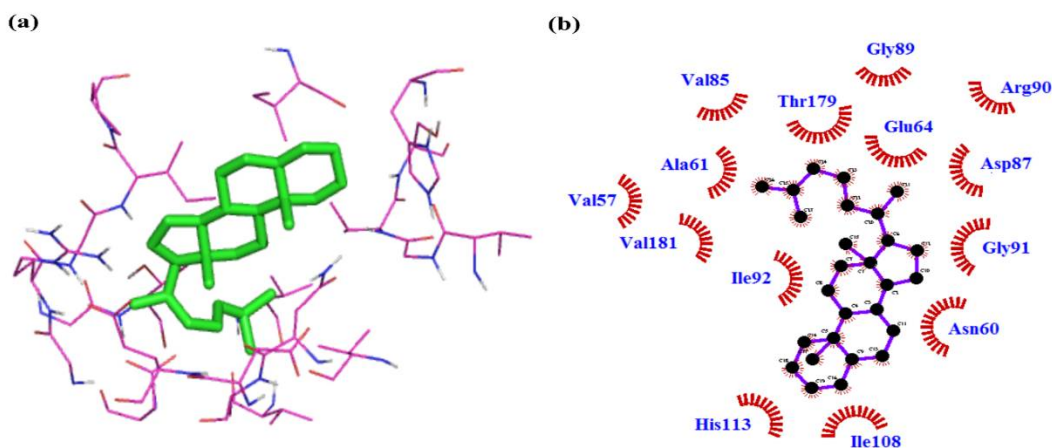


Figure 6. Docking results for DNA gyrase of *A. baumannii* and cholestane. (a) Binding mode of cholestane with the active site of DNA gyrase. Hydrogen bond interactions were not observed and the residues around the compound were highlighted. (b) Hydrophobic interactions of cholestane with DNA gyrase

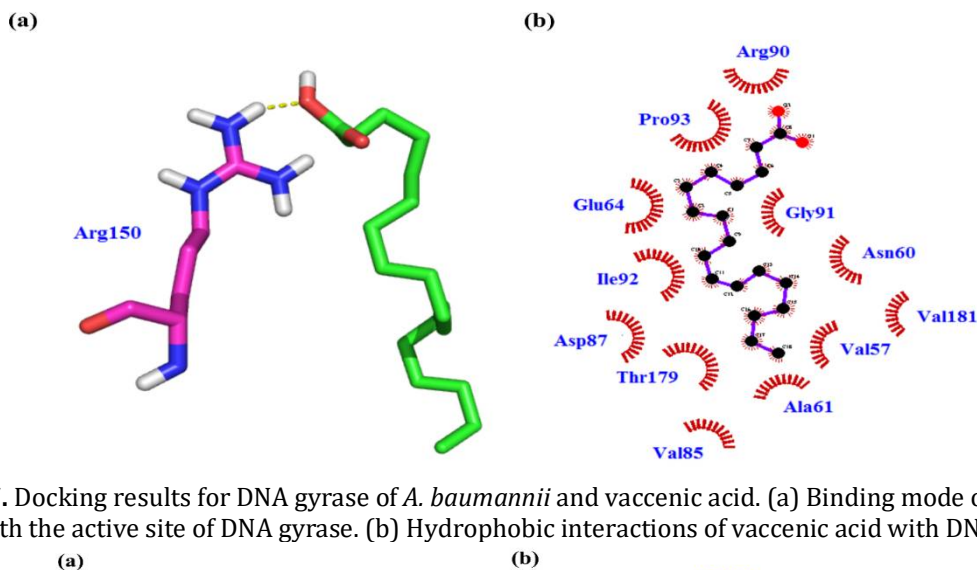


Figure 7. Docking results for DNA gyrase of *A. baumannii* and vaccenic acid. (a) Binding mode of vaccenic acid with the active site of DNA gyrase. (b) Hydrophobic interactions of vaccenic acid with DNA gyrase

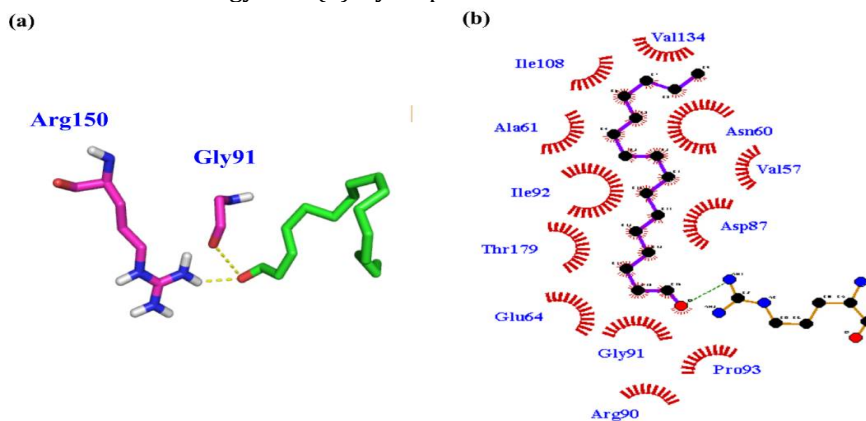


Figure 8. Docking results for DNA gyrase of *A. baumannii* and hexadecanal. (a) Binding mode of hexadecanal with the active site of DNA gyrase. (b) Hydrophobic interactions of hexadecanal with DNA gyrase

CONCLUSION

The potential of selected metabolites from the green seaweeds *Codium tomentosum* and *Ulva lactuca* to prevent biofilm formation was investigated. The target proteins for in silico molecular docking were Csue and DNA gyrase subunit B of *Acinetobacter baumannii*. The anti-biofilm and antimicrobial potential of seaweed metabolites was demonstrated by the docking energies of the metabolite cholestane, -10.25 kcal/mol for Csue and -9.55 kcal/mol for DNA gyrase B. The current study highlights the significance of edible green seaweed compounds in regulating the development of *Acinetobacter baumannii* biofilms. Future research would establish a promising seaweed-based strategy for inhibiting biofilm formation to control antibiotic resistance (AR).

ACKNOWLEDGEMENT

We sincerely thank King Institute of Preventive Medicine, NCR-SRMIST, and CIL-VISTA for microbial culture and analytical support.

CONFLICT OF INTEREST: The authors declare no conflicts of interest.

AUTHOR'S CONTRIBUTION

Mrs.Babini C K: Investigation, Methodology, Resources, analysis, and Writing - original draft.
 Dr. Reena A: Conceptualization, Validation, original draft, and Supervision.
 Dr. Malathi Kullappan: Technical support in analysis and Writing - original draft
 Dr. Krishna Mohan Surapaneni: Review and validation

FUNDING : This research work was not funded.

REFERENCES

1. Morris, F. C., Dexter, C., Kostoulias, X., Uddin, M. I., & Peleg, A. Y. (2019). The mechanisms of disease caused by *Acinetobacter baumannii*. *Frontiers in microbiology*, *10*, 1601.
2. Upmanyu, K., Haq, Q. M. R., & Singh, R. (2022). Factors mediating *Acinetobacter baumannii* biofilm formation: Opportunities for developing therapeutics. *Current Research in Microbial Sciences*, *3*, 100131.
3. Pompilio, A., Scribano, D., Sarshar, M., Di Bonaventura, G., Palamara, A. T., & Ambrosi, C. (2021). Gram-negative bacteria holding together in a biofilm: the *Acinetobacter baumannii* way. *Microorganisms*, *9*(7), 1353.
4. Ayobami, O., Willrich, N., Suwono, B., Eckmanns, T., & Markwart, R. (2020). The epidemiology of carbapenem-non-susceptible *Acinetobacter* species in Europe: analysis of EARS-Net data from 2013 to 2017. *Antimicrobial Resistance & Infection Control*, *9*(1), 89.
5. Jamal, Muhsina; Ahmad, Wisala; Andleeb, Saadiac; Jalil, Fazalb; Imran, Muhammad; Nawaz, Muhammad Asifd; Hussain, Tahira; Ali, Muhammadd; Rafiq, Muhammada; Kamil, Muhammad Atifb. (2018). Bacterial biofilm and associated infections. *Journal of the Chinese Medical Association* *81*(1):p 7-11. DOI: 10.1016/j.jcma.2017.07.012
6. Chen, C. L., Dudek, A., Liang, Y. H., Janapatla, R. P., Lee, H. Y., Hsu, L., ... & Chiu, C. H. (2022). d-mannose-sensitive pilus of *Acinetobacter baumannii* is linked to biofilm formation and adherence onto respiratory tract epithelial cells. *Journal of Microbiology, Immunology and Infection*, *55*(1), 69-79.
7. Pakharukova N, Tuittila M, Paavilainen S, Malmi H, Parilova O, Teneberg S, Knight SD, Zavialov AV. (2018). Structural basis for *Acinetobacter baumannii* biofilm formation. *Proc Natl Acad Sci U S A*. *22*;115(21):5558-5563. doi: 10.1073/pnas.1800961115.
8. Cotman, A. E., Durcik, M., Benedetto Tiz, D., Fulgheri, F., Secci, D., Sterle, M., ... & Kikelj, D. (2023). Discovery and hit-to-lead optimization of benzothiazole scaffold-based DNA gyrase inhibitors with potent activity against *Acinetobacter baumannii* and *Pseudomonas aeruginosa*. *Journal of medicinal chemistry*, *66*(2), 1380-1425.
9. Berman HM, Westbrook J, Feng Z, Gilliland G, Bhat TN, Weissig H, Shindyalov IN, Bourne PE. (2000). The Protein Data Bank. *Nucleic Acids Res*. *1*;28(1):235-42. doi: 10.1093/nar/28.1.235.
10. Kim HS, Jadhav JR, Jung SJ, Kwak JH. (2013). Synthesis and antimicrobial activity of imidazole and pyridine appended cholestane-based conjugates. *Bioorg Med Chem Lett*. *1*;23(15):4315-8. doi: 10.1016/j.bmcl.2013.05.098.
11. Shamsuzzaman, Khan MS, Alam M, Tabassum Z, Ahmad A, Khan AU. (2010). Synthesis, antibacterial and antifungal activities of 6,5 fused steroidal oxazoles in cholestane series. *Eur J Med Chem*. *45*(3):1094-7. doi: 10.1016/j.ejmech.2009.12.004.
12. Lin, C. Y., Huo, C., Kuo, L. K., Hiipakka, R. A., Jones, R. B., Lin, H. P., ... & Chuu, C. P. (2013). Cholestane-3 β , 5 α , 6 β -triol suppresses proliferation, migration, and invasion of human prostate cancer cells. *PloS one*, *8*(6), e65734.
13. Desai NC, Shihory NR, Kotadiya GM. Facile synthesis of benzimidazole bearing 2-pyridone derivatives as potential antimicrobial agents. *Chinese Chemical Letters*. 2014 Feb *1*;25(2):305-7.
14. Ponnuswamy S, Pushpalatha S, Akila A, Raghuvaman B, Aravindhana S. (2016). Synthesis, characterization, stereochemistry and antibacterial activity of N-acyl-2, 4, 6, 8-tetraphenyl-3, 7-diazabicyclo [3.3. 1] nonanes. *Journal of Molecular Structure*. *5*;1125:453-63.
15. Rajivgandhi, G. N., Ramachandran, G., Kanisha, C. C., Li, J. L., Yin, L., Manoharan, N., ... & Li, W. J. (2020). Antibiofilm compound of 1, 4-diaza-2, 5-dioxo-3-isobutyl bicyclo [4.3. 0] nonane from marine *Nocardia* sp. DMS 2 (MH900226) against biofilm forming *K. pneumoniae*. *Journal of King Saud University-Science*, *32*(8), 3495-3502.
16. Yazıcı A. (2024). The Strain-Dependent Antimicrobial and Antibiofilm effect of Cis and Trans-Vaccenic Acid against *Pseudomonas Aeruginosa*. *Cumhuriyet Science Journal*.*3*;45(1):1-7.
17. Karuppiyah V, Seralathan M. (2022). Quorum sensing inhibitory potential of vaccenic acid against *Chromobacterium violaceum* and methicillin-resistant *Staphylococcus aureus*. *World J Microbiol Biotechnol*. *27*;38(8):146. doi: 10.1007/s11274-022-03335-z.
18. El-Zairy AH, Mohamed HS, Ahmed SA, Ahmed SA, Okla MK, El-Adl K, AbdElgawad H, Hozzein WN. (2024). Spectroscopic analysis of wild medicinal desert plants from wadi sanor (beni-suef), Egypt, and their antimicrobial and antioxidant activities. *Heliyon*. *25*;10(21):e39612. doi: 10.1016/j.heliyon.2024.e39612.
19. Delnavazi,M.,Tavakoli,S.,Rustaie,A.,Batooli,H.,Yassa,N. (2014). Antioxidant and antibacterial activities of the essential oils and extracts of *Dorema ammoniacum* roots and aerial parts. *Research Journal of Pharmacognosy*, *1*(4): 11-18.
20. Alreshidi M, Badraoui R, Adnan M, Patel M, Alotaibi A, Saeed M, Ghandourah M, Al-Motair KA, Arif IA, Albulaihed Y, Snoussi M. (2023). Phytochemical profiling, antibacterial, and antibiofilm activities of *Sargassum* sp.(brown algae) from the Red Sea: ADMET prediction and molecular docking analysis. *Algal Research*. *1*;69:102912.
21. Gharaei S, Ohadi M, Hassanshahian M, Porsheikhali S, Foroootanfar H. (2022). Isolation, Optimization, and Structural Characterization of Glycolipid Biosurfactant Produced by Marine Isolate *Shewanella* algae B12 and Evaluation of Its Antimicrobial and Anti-biofilm Activity. *Appl Biochem Biotechnol*. *194*(4):1755-1774. doi: 10.1007/s12010-021-03782-8.

Copyright: © 2026 Author. This is an open access article distributed under the Creative Commons Attribution License, which permits unrestricted use, distribution, and reproduction in any medium, provided the original work is properly cited.